Study of Nearshore Sea Surface Features by the Navigational Radar Images

Li-Chung Wu* Laurence Zsu-Hsin Chuang** Chia Chuen Kao*** Jong-Hao Wang ****
* National Cheng Kung University / Coastal Ocean Monitoring Center, Tainan, Jack18@mail.ncku.edu.tw
** National Cheng Kung University / Institute of Ocean Technology and Marine Affairs, Tainan, zsuhsin@yahoo.com.tw
*** National Cheng Kung University / Department of Hydraulic and Ocean Engineering, Tainan, kaoshih@mail.ncku.edu.tw
**** Ministry of Economic Affairs / Water Resources Agency, Taipei, coal234s@yahoo.com.tw

Abstract

Ocean remote sensing is a useful way to obtain different information from sea surface. A large number of studies have proved the feasibility and accuracy on estimating different parameters of ocean waves by the nautical X-band radar technology. In addition to be an operational instrument for wave observations, the X-band radar is also a potential tool for the studies of nearshore physical processes. The aim of our study is to discuss the relationship between the X-band radar backscatter and different sea surface features within the surf zone. We found that the relationship between sea echo intensities and tidal features within the tidal inlet is obvious. Based on the spectral analysis of sea echo data within the tidal inlet, we could confirm the components of diurnal tide and semi-diurnal tide from the spectrum.

Keywords: Nearshore, X-band Radar, Remote Sensing

I. Introduction

Remote sensing should be one of the most popular means for monitoring ocean and coastal environments [1][2]. Satellite images have often been used for detecting and studying different ocean information. However, most of the satellites travel along their predetermined tracks, it is difficult to track the environmental features continuously. The sea surface observation by the X-band radar, a potential technology for obtaining continuous images of sea surface, was proposed several decades ago. The X-band radar is normally used to detect the coastline and obstacles on the sea surface. Due to the backscatter from the sea surface, it is currently one of the most useful tools for ocean remote sensing. Although the radar backscatter energy is not indicative of the elevation of sea surface level, it has been the most popular way to obtain near-wave field information both in time and space domains. It is also possible to monitor the same sea area continuously for the operational purpose. Spatio-temporal sea surface information can be acquired from continuous X-band radar images, which should be a significant tool for ocean monitoring.

The original idea on sea states observation by X-band radar can be traced back to Young et al. [3]. Following this research, some other studies proposed different algorithms to obtain the information of sea surface wind [4], current [5] and bathymetry [6] from the gravity wave patterns on the X-band

radar images. Note that these studies focus on the sea area images which are out of the surf zone.

In addition to be an instrument for wave, current and bathymetry observations, the X-band radar is also a potential tool for the studies of nearshore physical processes. The coastal sea surface phenomena often play key roles on coastal engineering and coastal management. They would be more complicated due to the influences of bathymetry, meteorological and marine factors. Because most of the nearshore sea surface features are distributed over a large-scale region in the spatial domain, the spatial characteristics of these phenomena should also be studied in greater detail. The aim of our study is to verify the practicability of X-band radar on detecting different sea surface phenomena nearshore. Radar image cases extracted from different sea areas will be applied to discuss the relationship between sea surface features and radar backscatter.

II. BCAKSCATTERING MECHANICS

In this section, we try to review the theories and mechanics of sea surface backscattering. The radar imaging mechanism from the sea surface is the Bragg resonant process, indicating the electromagnetic waves launched from radar antenna are strongly backscattered by ocean surface waves with half the electromagnetic wave length. To describe the interaction between the microwaves and the sea surface, Alpers et al. [7] revealed that radar sea-surface imaging mechanisms are dominated by the tilt (geometric) modulation and hydro-dynamic modulation of the backscatter. The tilt modulation is related to the slope of the sea-surface waves. For radar backscatter events in steep incidence areas, the utmost importance is given to direct reflection from large sea waves. In addition, high-frequency small-scale waves are influenced by large gravity waves through hydrodynamic modulation. Small-scale ripples are mostly situated on the front slopes of large-scale waves, next to their crests [8]. Within the surf zone, the mechanics of sea surface backscattering are more complicated due to the influences of breaking waves and other factors.

In addition to tilt modulation and hydrodynamic modulation, Seemann et al. [9] also proposed the existence of a shadowing effect during observation at a low grazing angle. A shadowing effect is a nonlinear imaging process for imaging wave patterns. Stevens et al. [10] reported the shadowing effect can actually obscure wave breaking on radar images. Sea surface radar images are generated by the interaction of electromagnetic waves with sea-surface ripples at grazing incidence. Although the backscatter energy from nautical X-band radar images is not indicative of the elevation of the sea surface, it has been a popular way to obtain near-wave field information. However, the radar backscatter is affected by shadowing, in which taller waves hide shorter waves from radar antenna illumination in the case of lower grazing incidence. Because of the shadowing effect, the radar backscatter intensity drops sharply. The waveform of the radar backscatter is neither smooth nor symmetrical, as in the waveform of a sine or cosine waveform; instead, it is skewed and asymmetrical. This phenomenon introduces additional frequency and wavenumber (spatial frequency) domain components to the radar image sequence spectrum. Because of the difference in the sea-surface wave forms between the deep-sea and shallow-water areas, the features of the shadowing effects from different wave forms should also differ.

III. STUDY SITE AND DATA FORMAT

To monitor coastal waters, we deployed a shore-based X-band navigational radar system at the western coast of Taiwan (23° 6.7900' N, 120° 3.1378' E), as shown in Figure 1. There is a lagoon in front of the radar antenna. Equipping with a 42 rpm antenna, the radar system has the frame

rate of 0.66 Hz and the range of 4.5 Km. The elevation of the radar antenna is about 20 m above the average water level. Either hourly or bi-hourly radar measurements have been conducted since September of 2010; the image cases consisting of 128 frames were used to our study. The X-band radar that is used in our study is a non-coherent system, which means that the information we need is only acquired from the radar echo intensity, and we do not process the phase information from the radar signals. As shown in Fig.2, we select four different sub-image cases from the whole sea surface image. Noting that sub-image case #3 is extracted from the surf zone. As we mentioned above, there is a lagoon within our radar monitoring area. The sub-image case #4 is extracted from tidal inlet area which connect the lagoon and sea area.

As mentioned above, every image case contains 128 continuous radar image sequences. The patterns of high frequency fluctuation, which are due to wind waves and swells, are often visible on the single frame image. To eliminate the spatial patterns of gravity waves from the sea surface images, we average the sequential images from 128 continuous image series. For each radar sub-image case, the intensities at a prescribed area consisting of 10 × 10 pixels were averaged and normalized by the image's maximum intensity. To analyze the radar backscatter from the averaged images, we normalize the radar echo intensity first as follows:

$$I_n(x,y) = I(x,y)/I_{\max} \quad (1)$$

where $I(x,y)$ is the original averaged radar echo intensity at different spatial locations (x,y), $I_n(x,y)$ is the normalized result from $I(x,y)$, and $I_{\max}$ is the maximal value of the entire $I(x,y)$. Note that the maximal values of the different image cases are always at the location of the radar antenna. Because all of the radar backscatter images are obtained from the same radar system, the values of $I_{\max}$ are also nearly the same among the different image cases.

Figure 1. The study site of radar experiment.

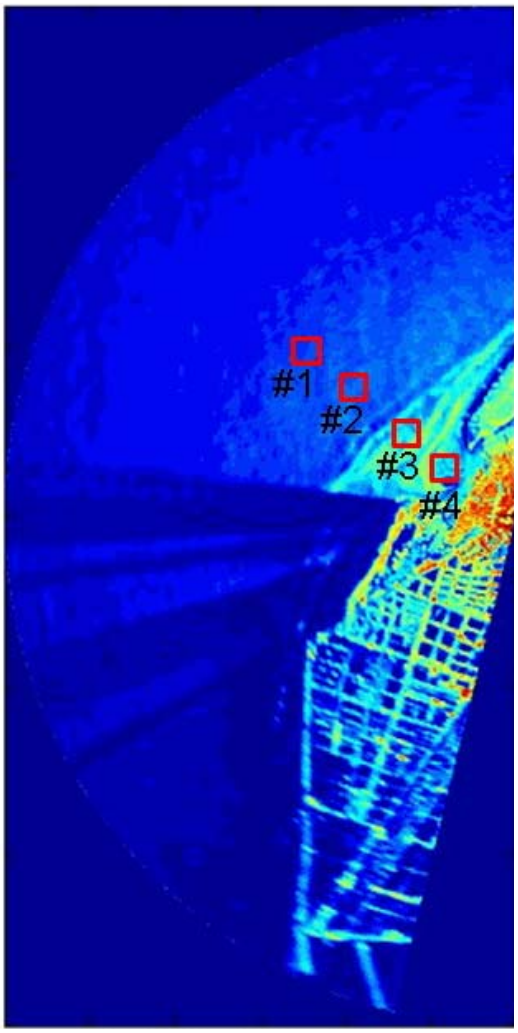

Figure 2. Locations of different radar sub-images.

With nearby ground-truth measurements of wind and waves on a data buoy, we have examined about 3,000 frames of radar image cases against the variations of these measured surface truth data. Although the distance between the locationsof the in-situ moored buoy and the radar monitoring area is approximately several kilometers, the wave data from the data buoy should still be useful for our study under the assumption of homogeneous sea states. The water depth of the buoy location is 17 m. In this sea area, the sea states are dominated by different monsoon systems. During the winter, the strong northeasterly wind has speeds as great as 19 m/s, which can induce wave heights of more than 3 m. Compared to the winter monsoon, the summer monsoon is much weaker and blows from the southwest. Additionally, the Taiwan Strait is located between the tropics and the subtropics and is sometimes influenced by typhoons.

IV. DATA ANALYSIS AND DISCUSSION

As shown in Fig.3, we discuss the relationship between in-situ wind speed and normalized radar backscatter intensity. The normalized radar backscatter intensities from different sub-image areas (cases #1 ~ case #4) on Fig.2 are used for the comparison. The results reveal the positive correlation between wind speed and normalized radar backscatter. We also notice that the correlation values from different sub-image cases are different. For the sub-image cases #1 and #2, the locations of these sub-image cases are often out of the surf zone. Sub-image case #2 shows higher correlation than other case. It should be noted that the distance between radar antenna and sub-image case #2 is larger than the distance between radar antenna and sub-image case #1. Nieto Borge and Guedes Soares [11] have reported that the radar image intensity is lower for larger distances because of the decay law for the received electromagnetic energy with distance. Due to the obvious influence of decay law on the case #1 radar backscattering, the correlation of case #1 between wind speed and normalized radar backscatter is lower than that of case #2. For the case #3 and case #4, these two areas are within the surf zone. Within this area, the radar backscattering is dominated by the phenomenon of wave breaking and also obvious tidal current from tidal inlet. Hence, the correlations of case #3 and case #4 between wind speed and normalized radar backscatter are also lower than the result of case#2. Especially for the correlations of case #4, it can hardly show the relationship between wind speed and radar backscatter. The similar phenomenon can also be discovered from the correlations between the in-situ wave height and normalized radar backscatter (Fig. 4). Comparing with Fig.3, the results of Fig.4 show higher correlation in case #3. Due to the influences breaking waves, the correlation between waves and radar backscatter is higher than the correlation between wind and radar backscatter. Besides, we also notice the relationship between wave height and radar backscatter is nonlinear.

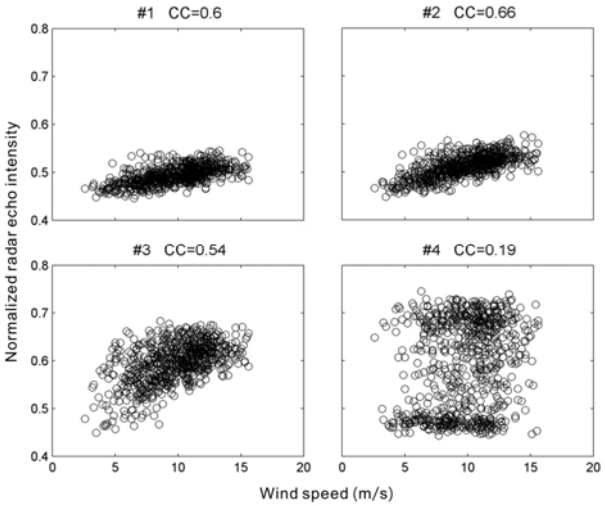

Figure 3. The relationship between radar backscatter and wind speed.

As we mentioned above, sub-image case #4 is extracted within tidal inlet. The relationship between tidal features and radar backscatter is also discussed in our study. Normalized intensities were

compiled against tidal levels. As shown in Fig. 1, there is a tidal station where is close to our study area. The distances between tidal station and radar sub-image location are all less than 20 km. Figure 5 presents the time series of normalized radar backscatter intensities and in-situ tidal level. The normalized radar backscatter intensities from sub-image cases #1~ #3 do not show obvious connection with the tidal level. However, we notice the oscillations of sub-image cases #4 are similar to the oscillations of in-situ tidal level. After the analysis of Fourier transform (Fig. 6), the spectra of sub-image cases #4 normalized radar backscatter intensities show two obvious energy peaks around the frequencies 1 (1/Day) and 2 (1/Day). Figure 6 reveals that the influences of diurnal and semi-diurnal tide upon the normalized radar backscatter intensities of the tidal inlet are quite obvious. In the near future, we will continue to study the mechanics of backscattering within the tidal inlet area.

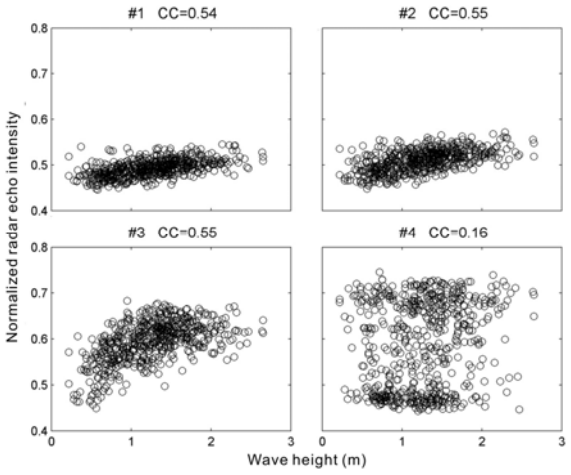

Figure 4. The relationship between radar backscatter and wave height.

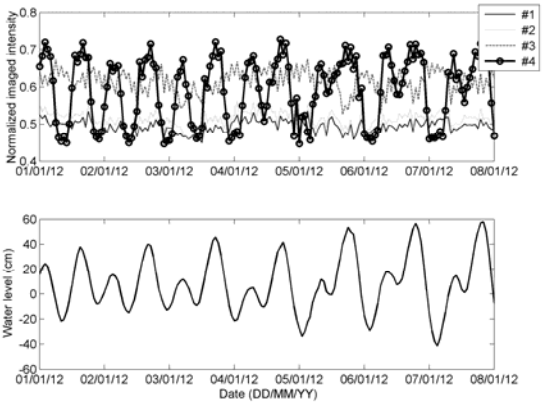

Figure 5. The relationship between radar backscatter and tidal level.

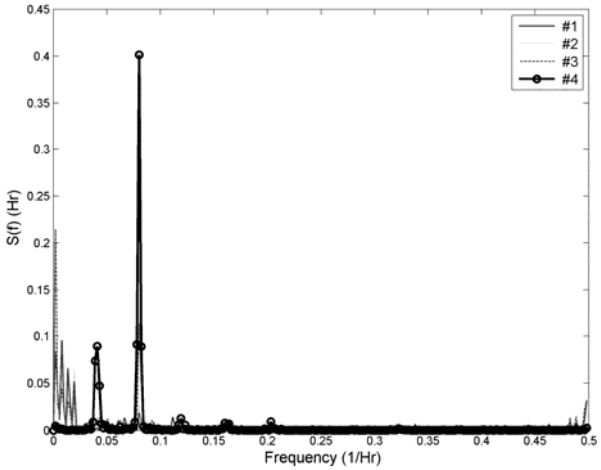

Figure 6. Spectra of radar backscatter.

V. SUMMARY

Since the 1980s, the X-band navigational radar has been proved its ability on ocean monitoring. Most of the studies applied this technology to study the sea surface area out of the surf zone, the application of X-band radar within the surf zone has received little attention. This study tries to discuss the relationship between the X-band radar backscatter from sea surface and different sea surface features within the surf zone. We revealed that wind, wave and tide are all dominate factors on radar backscattering. However, the influences of wind and waves are more obvious at the sea area out of the deeper sea area. On the contrary, the tidal features are more dominate within the tidal inlet area.

Acknowledgments

This research was supported by the National Science Council and the Water Resources Agency in Taiwan. The authors would like to offer their great thanks to these agencies.

References

[1] Pidgeon,V.W., 1968. Doppler dependence of radar sea return, *Journal of Geophysical Research*, Vol. 73, pp. 1333– 1341.

[2] Valenzuela, G.R., Laing, M.B., 1970. Study of Doppler spectra of radar sea echo, *Journal of Geophysical Research*, Vol. 75, pp.551–563.

[3] Young, I.R., Rosenthal, W., Ziemer, F., 1985. A three–dimensional analysis of marine radar images for the determination of ocean wave directionality and surface currents, *Journal of Geophysical Research*, Vol. 90, pp. 1049–1059.

[4] Dankert, H., Horstmann, J., 2007. A marine radar wind sensor, *Journal of Atmospheric and Oceanic Technology*, Vol. 24. pp. 1629–1642.

[5] Gangeskar, R., 2002. Ocean Current Estimated From X–Band Radar Sea Surface Images, *IEEE Transactions on Geoscience and Remote Sensing*, Vol. 40, No.4, pp. 783–792.

[6] Flampouris, S., Seemann, J., Senet, C., Ziemer, F., 2011. The Influence of the Inverted Sea Wave Theories on the Derivation of Coastal Bathymetry, *IEEE Geoscience and Remote Sensing Letters*, Vol. 8, No. 3, pp. 436–440.

[7] Alpers, W., Ross, D.B., Rufenach, C.L., 1981. On the detectability of ocean surface waves by real and synthetic aperture radar, *Journal of Geophysical Research*, Vol. 86, No. C7, pp. 6481–6498.

[8] Kanevsky, M.B., Radar Imaging of the Ocean Waves. Oxford: Elsevier, Ch. 2, pp. 9–24.

[9] Seemann, J., Ziemer, F., Senet, C.M., 1997. A method for computing calibrated ocean wave spectra from measurements with a nautical X–band radar, *OCEANS '97. MTS/IEEE Conference Proceedings*, Vol. 2, pp. 1148–1154.

[10] Stevens, C.L., Poulter, E.M., Smith, M.J., McGregor, J.A., 1999. Nonlinear features in wave–resolving microwave radar observations of ocean waves, *IEEE Journal of Oceanic Engineering*, Vol. 24, No. 4, pp. 470–480.